QUASAR OUTFLOWS AND ACTIVE GALACTIC NUCEUS FEEDBACK: ANALYSIS OF QSO J1509+2432

Doyee Byun
Department of Physics, Virginia Tech, Blacksburg, VA, 24061
(Advisor: Nahum Arav)

Abstract

We analyze the spectrum of quasar QSO J1509+2432 to find the physical conditions of its outflow. The analysis is based on the data from the Very Large Telescope/Ultraviolet and Visual Echelle Spectrograph, with an observed wavelength range of 3000 to 9500 Å. The outflow system of interest travels at ~1700 $\mathrm{km\ s^{-1}}$ away from the central source. We have detected absorption troughs of ions Si II and O I, and measured their column densities. In our attempt to find the electron number density of the outflow system from the ratio between the excited and ground state column densities of Si II and O I, we have found that they would each give different results of $\log(n_e) \approx 3$ for Si II, and $\log(n_e) \approx 7.5$ for O I, without a clear method to resolve this contradiction.

1. Introduction

Quasars are extremely luminous active galactic nuclei (AGN), with a luminosity larger than $10^{45}\mathrm{erg\ s^{-1}}$. They are energized from material accretion into the supermassive blackhole in the nucleus, with high luminosity across the electromagnetic spectrum caused by a release of gravitational potential energy, as well as friction (Lynden-Bell, 1969; Shields, 1999).

Roughly 40% of quasars have outflows, which are materials flowing away from the center of the quasars. They are shown in their spectra as troughs "blue-shifted" relative to redshifted emission features. A wide variety of outflows exist, such as molecular, atomic, ionized, and X-ray outflows (Hewett & Foltz, 2003; Dai et al, 2008; Krips et al, 2011; Feruglio et al, 2015; Kanekar & Chengalur, 2008; Aditya & Kanekar, 2018; Korista et al, 2008; Shen et al, 2011; Chartas et all, 2009; Tombesi et al, 2015). These outflows can potentially produce AGN feedback, interactions between the AGN and host galaxy via the outflow mechanical energy that involve the restriction of the growth of the host galaxy, the correlation between the mass of the central black hole and the galactic bulge, and the chemical enrichment of the intracluster and intergalactic medium.

Outflows are estimated to need to have a kinetic luminosity of at least 0.5~5% of the quasar's Eddington luminosity to contribute to AGN feedback. (Scannapieco, 2004; Di Matteo et al, 2005; Hopkins & Elvis, 2010; Fiore et al, 2017; Arav et al, 2020). A distribution of kinetic and bolometric luminosities of outflows can be found in Figure 1 of Miller et al, 2020.

In order to find whether a quasar's outflow system has enough kinetic luminosity to contribute significantly to AGN feedback, we employ an analysis method that involves spectrum analysis and measurement of ionic column densities of the outflow system. With the measured column densities, we find the hydrogen column density and ionization parameter using spectral synthesis code Cloudy (c17.00, Ferland et al, 2017). With knowledge of these parameters, along with the electron number density, calculated from the ratio between excited and ground state column densities of selected ions, we find the distance of the outflow system from the central source, and ultimately, the kinetic luminosity of the system. This systematic approach has yielded notable results in the past (see Xu et al, 2018; Miller et al, 2018; Arav et al, 2020; Miller et al, 2020b).

We have analyzed the outflow of the quasar QSO J15092338+2432433 (hereafter QSO J1509+2432) in order to find its energetics parameters, such as distance to the central source, mass flow rate, kinetic luminosity. This was to find whether the kinetic luminosity was large enough compared to the Eddington luminosity of the quasar for the outflow to contribute significantly to AGN feedback.

The structure of the paper is as follows. Section 2 describes the observation of QSO J1509+2432, and the spectral fitting for continuum and emission lines. Section 3 details the analysis performed on the spectrum, such as the measurement of ionic column densities, as well as our reasoning for our focus on two particular ions, Si II and O I. Section 4 discusses the discrepancies and roadblocks that prevented us from reaching a definitive result for the energetics parameters. Section 5 closes the paper with a summary and conclusion.

2. Data Retrieval and Spectral Fitting

QSO J1509+2342 (J2000: RA = 15:09:23.38, decl. = +24:32:43.3, redshift z = 3.06133) was observed in April 2009 with the Very Large Telescope (VLT) Ultraviolet and Visual Echelle Spectrograph (UVES) as part of the program 083.B-0604 (PI: Benn).

We have retrieved the observational data from the European Southern Observatory database, the plot of which can be found in Figure 1. We then identified a narrow absorption system traveling ~1700 km s^{-1} away from the central source by matching known wavelengths of absorption lines to the spectrum at z = 3.03853. We have also modeled the quasar’s continuum using a power law, and the emission lines using Gaussians. The spectrum with the absorption system identified, as well as the continuum and emission model, can be seen in Figure 2.

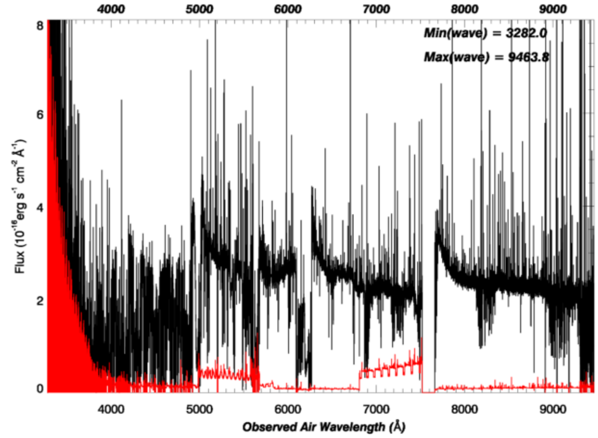

Figure 1. Spectrum plot of QSO J1509+2342. Black line is the flux signal, red is the reported error.

3. Data Analysis

3.1 Si II and O I: distance diagnostics

We focus on Si II and O I for this analysis, as the existence of excited state absorption troughs make them suitable candidates for finding the distance of the outflow system from the central galactic source, the method of which will be detailed in 3.3. Plots of the Si II and O I troughs in velocity space are shown in Figure 3.

3.2 Ionic column densities

From the Si II and O I troughs that have been identified, we have computed the ionic column densities of the ground and excited states using the apparent optical depth (AOD) (Savage & Sembach, 1991; Arav et al, 2001) and partial covering (PC) methods (Arav et al, 2005; Miller et al, 2018).

The AOD method assumes a homogeneous outflow that completely covers the central source. While this assumption is convenient for a simple method of calculating the column density, the computation result can be underestimated relative to the true physical value due to being unable to take effects such as non-black saturation into account. This can be addressed with the PC method, that assumes that the outflow only covers a portion

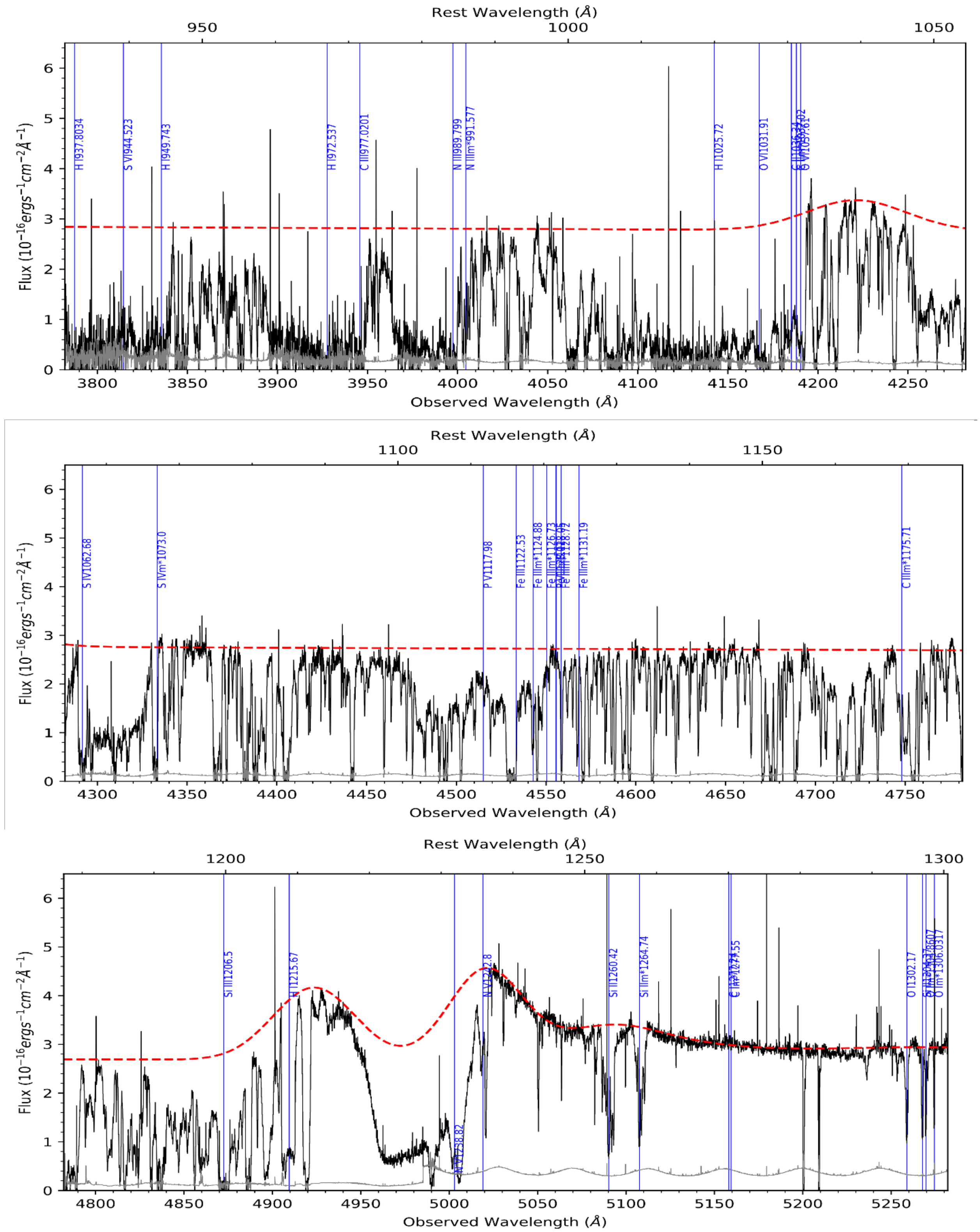

Figure 2. Enlarged spectrum plot of QSO J1509+2342. The black curve represents the flux, the gray curve represents the reported error in the flux, and the red dashed curve represents the continuum and emission model. The blue vertical lines are the locations of absorption lines for the absorption outflow system. Note the S II absorption lines at ~5100 Å and the O I absorption at ~5250 Å.

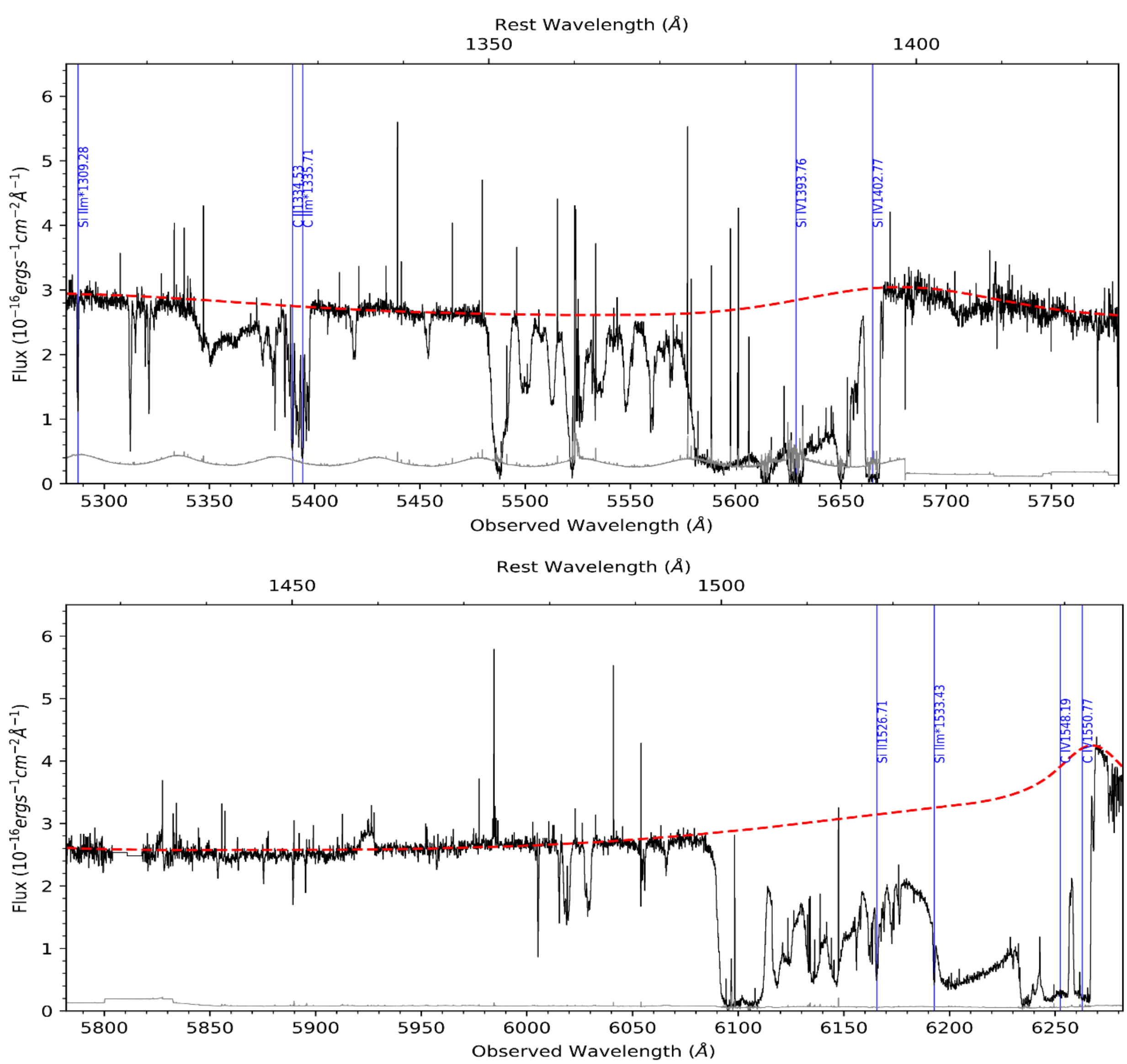

Figure 2 cont.

of the source. While this can give a more accurate value of the column density, it is limited in that it requires a doublet absorption line to be viable.

The measured column densities of the Si II and O I absorption lines are shown in Table 1.

3.3 Electron number density

Calculating the electron number density of the outflow system is crucial to finding its distance from the central source. This is due to the relation between the distance and hydrogen number density that can be found in the ionization parameter equation found in Equation 3 of Borguet et al, 2012:

$$U_H = \frac{Q_H}{4\pi R^2 n_H c} \quad (1)$$

where U_H is the ionization parameter, Q_H is the ionizing photon emission rate, c is the speed of light, R is the distance of the outflow from the central source, and n_H is the hydrogen number density. The hydrogen number density and electron number density are directly proportional such that the electron number density $n_e \cong 1.2\, n_H$ in a highly

Troughs	oscillator strength	AOD	PC
Si II (1260 and 1304)		170^{+20}_{-10}	210^{+40}_{-20}
Si II 1260	1.22	$30^{+2.4}_{-1.8}$	
Si II 1304	9.28×10^{-2}	170^{+20}_{-10}	
Si II 1808	2.49×10^{-3}	3890^{+930}_{-680}	
Si II* 1264	1.09	20^{+3}_{-2}	
Si II* 1265	1.13×10^{-1}	120^{+20}_{-10}	
Si II* 1309	8.00×10^{-2}	120^{+20}_{-20}	
Si II* 1817	1.97×10^{-3}	1150^{+650}_{-470}	
O I 1302	5.20×10^{-2}	340^{+40}_{-30}	
O I* 1304	5.18×10^{-2}	210^{+30}_{-20}	
O I* 1306	5.19×10^{-2}	100^{+20}_{-20}	

NOTE—Units are in $10^{12}\mathrm{cm}^{-2}$.

Table 1. Measured column densities of Si II and O I lines of QSO J1509+2342. The numbers next to the name of the ions in the "Troughs" column are the wavelengths of the absorption lines in Angstroms. The oscillator strengths of lines are a parameter indicating the likelihood of a particular transition occurring. The AOD and PC columns show the column densities measured using the apparent optical depth and partial covering methods, respectively. Note that the measured column densities differ significantly from trough to trough, even for identical states of the same ion. This can be attributed to a combination of differing oscillator strengths, as well as some of the absorption lines potentially having been highly saturated.

ionized plasma (Chamberlain & Arav, 2015), so once we find estimates for the electron number density, the ionization parameter, and the ionizing photon emission rate, we can find the distance of the outflow.

The computation of the electron number density is done as follows. After choosing an ion for which both a resonance state and excited state absorption is detected, we use the CHIANTI atomic database (version 10, Dere et al, 1997; Del Zanna et al, 2021) to find the relation between the electron number density, and the ratio between the excited and resonance state abundances. With the measured column densities of the excited and resonance states, we then find the ratio between the two states within the system, and find which electron number density value that this ratio corresponds to. This method is demonstrated in Arav et al, 2013; Chamberlain & Arav 2015; Xu et al, 2018; and Miller et al, 2020b.

To gain a ballpark estimate of the electron number density, we referenced the population ratio plots produced by Ding 2019 in order to match the ratio of excited and ground state populations of Si II and O I to their corresponding electron number densities (See Figure 4). As can be seen in the plots, the values of n_e given by Si II and O I are $\log(n_e) \approx 3$ and $\log(n_e) \approx 7.5$ respectively.

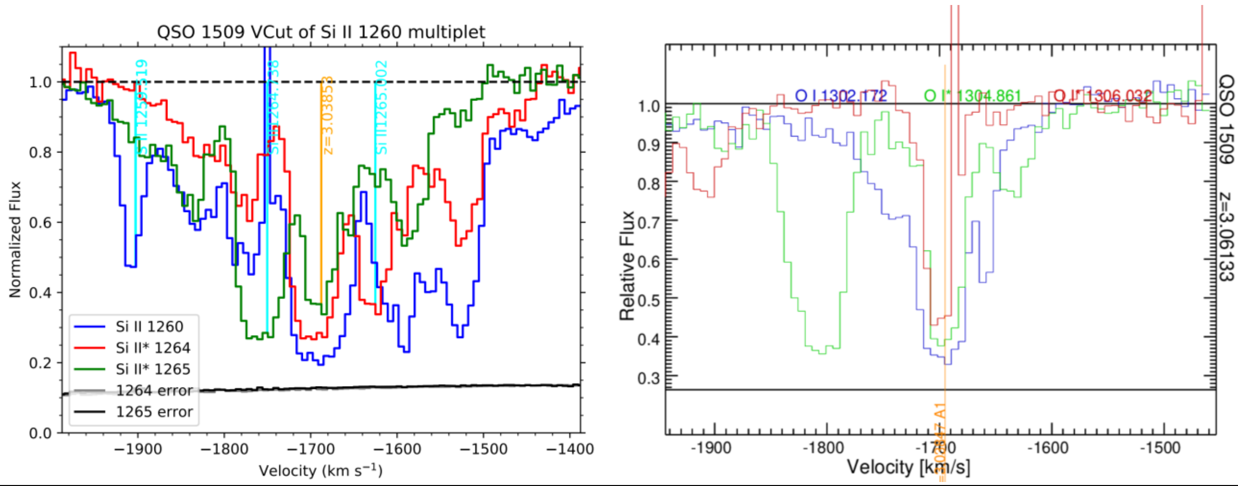

Figure 3. (left) Plot of Si II absorption troughs of the 1700 $km\ s^{-1}$ outflow system in velocity space. The orange vertical line indicates the location of the outflow system in velocity space. The cyan vertical lines touching the red, blue, and green curves show the locations of absorption troughs of different wavelengths on their respective curves. (right) Plot of O I absorption troughs in velocity space. The blue, green, and red curves show the O I 1302.172, O I* 1304,861, and O I* 1306.032 troughs, respectively.

4. Discussion

As mentioned in 3.3, the value of n_e found using Si II and O I differ by more than four orders of magnitude, a discrepancy too large to attribute simply to measurement uncertainties. This could be explained by high saturation of absorption troughs, but without a clear way to find which troughs are saturated, we are unable to resolve the contradiction.

Without a way to move forward in the analysis of this object, we have decided to move onto examining other objects that have been observed with the VLT. The sample we are now focusing on is the UVES Spectral Quasar Absorption Database (SQUAD, Murphy et al, 2019), which contains high resolution spectra of 467 quasars, with a median signal-to-noise ratio of 20. We expect to find quasars with outflow systems from this sample of hundreds, and to find their physical characteristics.

One such characteristic would be the distance of the outflows from their central sources, and we expect S IV absorption troughs to be a useful distance diagnostic, using the method described in 3.3. S IV is the only high ionization species with an observable excited state, and has been used as a distance diagnostic in ground-based analysis with successful results (Xu et al, 2018).

5. Summary and Conclusion

Quasar outflows can potentially contribute to AGN feedback depending on how large their kinetic luminosities are relative to the Eddington luminosities of the quasars. Whether outflows meet the luminosity criteria can be found via the analysis method described in 1 and 3, in a systematic and methodical manner. However, as discussed in 4 for QSO J1509+2342, there are limitations to what can be achieved through this method that depend on the quality of the spectrum data itself, as well as the consistency of the depth of the absorption troughs.

To find objects more suitable for this analysis method, we will examine the SQUAD data release published by Murphy et al, 2019. We expect to find more substantial results from this sample.

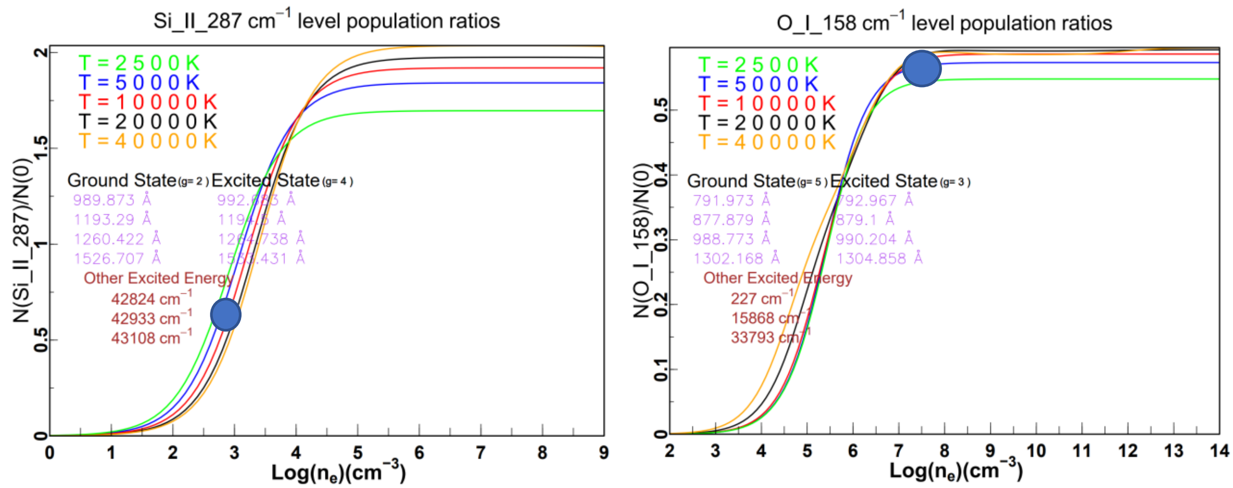

Figure 4. Si II and O I population ratio vs electron number density plots at T=2500, 5000, 10000, 20000, 40000K, adapted from Ding, 2019. The Si II ratio (0.57) was found using the partial covering column density of the 1260 and 1304 Å doublet, and the column density of the 287 cm^{-1} level excited state trough. The O I ratio (0.61) was found using the AOD column density of the 1302 Å resonance line, and the 158cm^{-1}excited state column density. The found ratios and electron number densities are marked with blue circles.

Acknowledgements

This research has been supported by the Virginia Space Grant Consortium Graduate Fellowship.

References

Aditya, J.N.H.S, Kanekar, N., 2018, MNRAS, 481, 1578
Arav, N. et al, 2001, ApJ, 546, 140
Arav, N. et al, 2005, ApJ, 620, 665
Arav, N. et al, 2013, MNRAS, 436, 3286
Arav, N. et al, 2020, ApJS, 247, 37
Borguet, B.C.J. et al, 2012, ApJ, 751, 107
Chartas, G. et al, 2009, ApJ, 706, 644
Dai, X. et al, 2008, ApJ, 672, 108
Di Matteo, T. et al, 2005, Nature, 433, 604
Ding, Z., 2019, "Level Population Ratios", http://www1.phys.vt.edu/quasar/edmonds/stuff/
Ferland, G.J. et al, 2017, RMxAA, 53, 385
Feruglio, C. et al, 2015, A&A, 583, A99
Fiore, F. et al, 2017, A&A, 601, A143
Hewett, P.C., Foltz, C.B., 2003, AJ, 125, 1784
Hopkins, P.F., Elvis, M., 2010, MNRAS, 401, 7
Kanekar, N., Chengalur, J.N., 2008, MNRAS,
Korista, K.T. et al, 2008, ApJ, 688. 108
Krips, M. et al, 2011, ApJ, 736, 37
384, L6
Lynden-Bell, D., 1969, Nature, 223, 690
Miller, T.R. et al, 2018, ApJ, 865, 90
Miller, T.R. et al, 2020a, MNRAS, 499, 1522
Miller, T.R. et al, 2020b, ApJS, 247, 39
Murphy, M.T. et al, 2019, MNRAS, 482, 3458
Savage, B.D., Sembach, K.R., 1991, ApJ, 379, 245
Scannapieco, E., Oh, S.P., 2004, ApJ, 608, 62
Shen, Y. et al, 2011, ApJS, 194, 45
Shields, G. A., 1999, PASP, 111, 661
Tombesi, F. et al, 2015, Nature, 519, 436
Xu, X. et al, 2018, ApJ, 858, 39